Parameters of solar wind electron heat-flux pitch-angle distributions and IMF topologies

W. M. Feuerstein, D. E. Larson, J. G. Luhmann, and R. P. Lin
Space Sciences Laboratory, University of California, Berkeley, California, USA

S. W. Kahler
Air Force Research Laboratory, Space Vehicles Directorate, Hanscom Air Force Base, Massachusetts, USA

N. U. Crooker
Center for Space Physics, Boston University, Boston, Massachusetts, USA

Received 14 May 2004; revised 18 October 2004; accepted 27 October 2004; published 23 November 2004.

[1] Pitch-angle distributions (PADs) of solar wind heat-flux (HF) electrons are used as a proxy for interplanetary magnetic field (IMF) topology. Unidirectional PADs yield IMF solar polarities, and bidirectional electron (BDE) PADs are interpreted as signatures of closed fields. A general perception exists that the directionalities are easily distinguished, clearly defining open and closed IMFs. We quantify PADs with the ratios of the HF parallel and antiparallel to the IMF to that perpendicular to the IMF plotting these parameters against each other in a directionality distribution for six years of electron data from the 3DP experiment on the *Wind* satellite. This bimodal plot clearly shows the unidirectional populations, but shows no evidence for a separate bidirectional HF population. A similar plot of magnetic clouds is double-banded with no evidence of a bifurcation between bidirectional and unidirectional regimes. In conclusion, this basic parameterization shows no distinction between open and closed field topologies. *INDEX TERMS:* 2134 Interplanetary Physics: Interplanetary magnetic fields; 2164 Interplanetary Physics: Solar wind plasma; 2169 Interplanetary Physics: Sources of the solar wind; 7513 Solar Physics, Astrophysics, and Astronomy: Coronal mass ejections; 7524 Solar Physics, Astrophysics, and Astronomy: Magnetic fields. **Citation:** Feuerstein, W. M., D. E. Larson, J. G. Luhmann, R. P. Lin, S. W. Kahler, and N. U. Crooker (2004), Parameters of solar wind electron heat-flux pitch-angle distributions and IMF topologies, *Geophys. Res. Lett.*, *31*, L22805, doi:10.1029/2004GL020529.

1. Introduction

[2] Global IMF topology is important to understanding solar magnetic field evolution. Since energetic charged particles emitted by the Sun are constrained to follow individual lines of the IMF, they have been used extensively as probes of the IMF topology and polarity. Early work by *Marsden et al.* [1987] and *Gosling et al.* [1987] with counterstreaming flows of solar E > 80 eV electrons (previously called bidirectional electron events) and E > 35 keV protons, respectively, first comprehensively treated closed IMFs. Comparing the flow directions of solar E > 2 keV electrons relative to the local IMF directions to determine the IMF polarities, *Kahler and Lin* [1994, 1995] explored the relationship between those IMF polarities and the IMF sector boundaries determined solely from the IMF directions.

[3] The subsequent use of nearly ubiquitous solar wind E $\geq$ 80 eV heat-flux (HF) electron [*Feldman et al.*, 1975; *Marsch*, 1991] observations allowed the statistical examination of IMF polarities over periods of years on time scales as short as minutes to tens of minutes [e.g., *Kahler et al.*, 1998]. The counterstreaming HF electron (CSE) flows have now been the basis of many studies of Interplanetary Coronal Mass Ejections (ICMEs) [e.g., *Gosling et al.*, 1987, 1992; *Crooker et al.*, 1998a, 1998b; *Kahler et al.*, 1999; *Shodhan et al.*, 2000; *Gosling and Forsyth*, 2001]. In addition, HF electron dropouts [e.g., *McComas et al.*, 1989; *Crooker et al.*, 1996; *Larson et al.*, 2000; *Collier et al.*, 2001] have been used as a signature of disconnected IMF topologies. Thus, the HF electron PADs are now an important tool to deduce the topology and dynamics of the IMF.

[4] Though they are crucial for our understanding of the IMF topology, the selection and interpretation of HF electron signatures have been based on qualitative assessments of PADs. Color-coded PAD intensity plots showing clear cases of CSEs [e.g., *Gosling et al.*, 1987; *Reisenfeld et al.*, 2003] have been published, but without accompanying quantitative criteria for their selection. This is somewhat justified since there are as yet no quantitative models to relate PADs to particular IMF topologies, and nonsolar sources of E $\geq$ 80 eV electrons, such as the Earth's bow shock and interplanetary shocks [*Tsurutani and Lin*, 1985], can present misleading contributions to the HF electron PADs. However, important quantitative estimates of the fraction of closed versus open IMF lines (i.e., resolving the flux catastrophe problem [*McComas et al.*, 1989; *Gosling et al.*, 1992; *Shodhan et al.*, 2000]) are based on the above qualitative analyses.

[5] With only several basic topologies and geometries for the IMF, one might expect that synoptic plots of appropriately defined HF electron PAD parameters will define the signatures of those topologies and allow us to make quantitative estimates of their occurrences in time. In particular, one may expect to find separate populations for the basic open and closed IMFs. Here the authors present an

0094-8276/04/2004GL020529$05.00

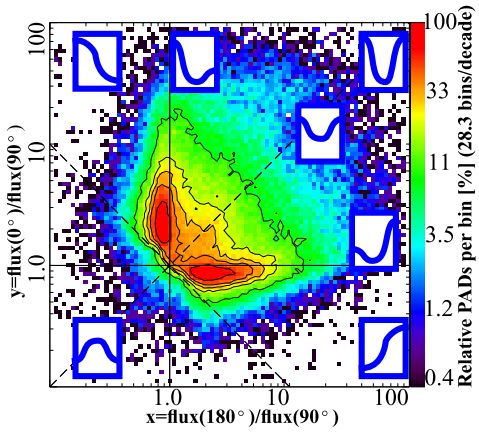

Figure 1. Directionality distribution of the entire unfiltered data set with seven schematics overlaid each representing flux vs. PA from 0 to 180 (left to right). The schematics qualitatively show the plot positions for various kinds of PADs. See text for an explanation of the distribution.

analysis of HF electron PAD data to look for signatures of the different topologies.

2. Methodology and Data Analysis

2.1. The Full 3DP Data Set

[6] The data are from the 3-D Plasma and Energetic Particle Experiment (3DP) [*Lin et al.*, 1995], which provides observations of electrons from ~10 eV to ~300 keV at the Wind spacecraft. 3DP samples flux in all directions in eighty-eight approximately equal solid angle bins. A pitch angle (PA) bin is the average of all solid angle bins within 22.5° of the PA center. The IMF observations are obtained from the Magnetic Field Investigation (MFI) [*Lepping et al.*, 1995] on Wind. This work studies ~350 eV electrons which are usually representative of the directionality of the entire halo population. We resample the data to 15-minute averages from November 14, 1994 to December 1, 2000.

[7] To characterize each PAD by two parameters and indicate its directionality and degree of anisotropy, the relative fluxes at three PAs (0°, 90°, and 180°) are used. One can define x as the ratio of the flux at 180° to the flux at 90° and y as the ratio of the flux at 0° to the flux at 90°. Each 15-minute PAD is then represented as a single point on a log x-log y plot, as expressed in the plot and caption of Figure 1. The position of the point uniquely describes the basic shape, and thus the directionality, of the PAD. The four regimes of directionality (unidirectional-positive, where $y \geq 1$ and $x \leq 1$; unidirectional-negative, where $y \leq 1$ and $x \geq 1$; counterstreaming, or CSE, where $y > 1$ and $x > 1$; and the predominantly perpendicular, where $y < 1$ and $x < 1$) make up the directionality plot. We see two ridges in the unidirectional regimes, and a slight enhancement along y = x within the CSE region.

[8] To investigate the origin of the enhancement we choose to eliminate intervals when *Wind* is magnetically connected to Earth's bow shock, since these events are a known source of non-heliospheric CSEs [*Stansberry et al.*, 1988]. An algorithm that calculates 15-minute averages of the IMF direction at Wind and projects the model IMF line onto a model Earth bow shock is used to delete all data during and within ten minutes of periods of calculated magnetic connections. The additional deletion of data periods when WIND was less than 60 $R_\oplus$ from Earth results in a total elimination of 45.7% of the original 212,064 PADs.

[9] Figure 2 shows the plot of the remaining PADs mostly free of magnetic connection to the bow shock (note that a complete data cleaning is very difficult [*Stansberry et al.*, 1988]). Note the prominent ridges of the unidirectional legs along $x \sim 0.8$ (positive polarity fluxes) and $y \sim 0.8$ (negative polarity fluxes) that signify the expected predominance of typical unidirectional fluxes in normal solar wind conditions. Points near y = x have nearly symmetric CSE fluxes. Points near x, y = 1 are close to isotropy and those in the region $x, y \geq 1$ represent CSE PADs. The CSE PADs close to the high unidirectional ridges are only weakly counterstreaming (i.e., very close to the boundary of the counterstreaming region). The densities are plotted logarithmically, so the overall CSE density is much weaker than that of the unidirectional peaks. The whole CSE population is widely spread out and shows no indication of a separate population(s) of CSEs, contrary to our expectation based on the assumption that the points in the directionality plots should reflect the two distinct open and closed IMF topologies.

2.2. A Selected Magnetic-Cloud Data Set

[10] In an attempt to identify a distinct population of CSE events a set of 20 magnetic clouds (MCs) were selected from the observations distinguished by a key signature not involving HF electrons - strong, low-variance rotating magnetic fields [*Burlaga*, 1991]. MCs generally exhibit a high degree of CSEs, suggesting they are largely topologically closed [*Shodhan et al.*, 2000], and therefore serve as guides for determining the characteristic directionality-plot signatures of closed topologies. Figure 3 is the directionality plot of the 20 MCs, where the data points are a small subset of Figure 2. Note a dearth of PADs near the y = x line. Most of the PADs along that line in Figure 3 are due only to a single MC. The dominant feature is the suggestion of two broad bands, or ridges, roughly parallel to but

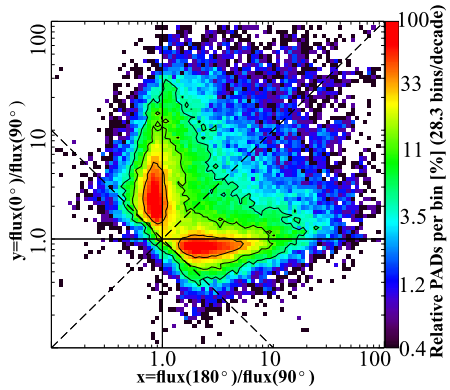

Figure 2. Directionality distribution for the full data set after filtering out bow shock connected PADs. The density enhancement along y = x, found in Figure 1, is not observed.

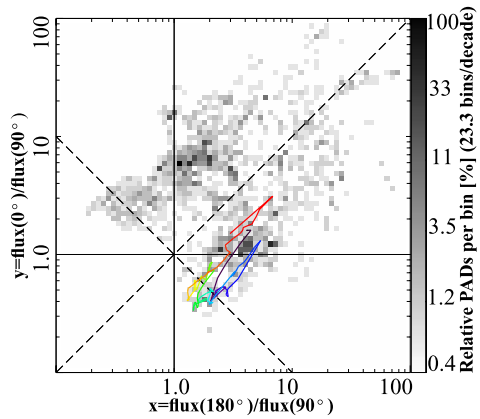

Figure 3. Directionality distribution for 20 MCs selected from the full data set on the basis of low variance rotating magnetic fields. The bands span the counterstreaming and unidirectional regimes. The color trace shows the chronological (blue to red) time evolution of a particular magnetic cloud.

displaced from the y = x line. The peaks of those bands lie within the counterstreaming regime where x/y or y/x $\sim$ 3–4. As expected for closed field topologies characteristic of MCs, most of the PADs, including the peaks, lie in the counterstreaming regime. However, many MC PADs are also found in the unidirectional regimes, and no feature (e.g., local extremum, or discontinuity) is observed that would indicate multiple populations along each band and/or a natural division of PADs into distinct regimes.

[11] Plots of individual MCs generally show points lying predominantly on one side of the y = x line, indicating that the cause of the skewing does not change during the event. In a number of cases, the data points move smoothly in time across the boundaries of the unidirectional/counterstreaming regimes, sometimes both out of and back into the counterstreaming regime. The evolution of points in some MCs is a trace or ridge strikingly parallel to the y = x line (see overlaid color trace in Figure 3, and the caption, for an example). Parallels to y = x indicate that the ratio of 0° to 180° fluxes remains fairly constant while the parallel-to-perpendicular anisotropy varies over time. In such cases, the perpendicular flux generally varies while the sum of the parallel fluxes remains constant.

3. Discussion

[12] The directionality distribution of Figure 2 clearly shows the two anticipated unidirectional HF electron PAD peaks, but no sign of a third peak (of any shape or location) of counterstreaming PADs that one may associate with topologically closed IMFs. The absence of a peak is worthy of discussion. Figure 1 shows that the plotting method is indeed effective at revealing the population of bow shock connection PADs. Perhaps the peak is smaller than the enhancement of Figure 1 and/or too spread out to be observed. The PADs of Figure 2 were also plotted in another format with x/y versus x - y. This format would map all points near the y = x line of Figure 2 to near the point (0, 1), perhaps showing a peak not obvious in Figure 2. Since that format also reveals no separate population, the absence of a third peak is likely not an artifact of the directionality plot format. A second possibility for the failure to find a third peak is that analyzing only three PAs (0°, 90°, and 180°) is overly restrictive. A more general parameterization of 3DP PADs by *Kahler et al.* [2003] fits the full PAD (i.e., $I(\theta = \mathrm{PA})$) to the Fourier cosine harmonics $\log I(\theta) = A_0 + A_1\cos(\theta) + A_2\cos(2\theta) + A_3\cos(3\theta)$, where the A_2 term is the key diagnostic for CSE events. They find no obvious quantitative criteria for selecting CSE periods. Previous work to detect counterstreaming protons and ions in the IMF by *Marsden et al.* [1987], *Richardson and Reames* [1993], and *Richardson et al.* [2001] imposed arbitrary requirements for the A_n to define counterstreaming, but their reliance on the A_2 term is very similar to this study's restriction to the PAs of 0°, 90°, and 180°. The selection of counterstreaming periods from PAD plots by eye also uses subjective criteria (such as a depressed 90° PA intensity) close to those discussed here. Thus the use of only three PAs does not appear to account for the absence of a counterstreaming peak in Figure 2.

[13] Directionality plots of the best candidates for closed IMFs show two broad bands in the counterstreaming regime parallel to, and on either side of, the y = x line and extending into the unidirectional regimes (Figure 3). An MC PAD trajectory along the band toward smaller x and y corresponds to an increasing isotropy of the PAD with a fixed ratio of the 0° flux to the 180° flux. Such behavior may reflect properties of the IMF topology, but *Crooker et al.* [2003] have shown that the HF electron isotropies correlate well with the local plasma ion β parameter. Since MCs are defined in part by low β plasmas [*Shodhan et al.*, 2000], the MC PADs may lie in the counterstreaming region not because of their IMF topologies, but rather because of their characteristic low β. Note that the y/x ratio of the positive polarity flux peak and the x/y ratio of the negative polarity flux peak of Figure 2 are about the same as those of the corresponding peaks of Figure 3 (about 3 to 4 in both cases). Thus, a decrease in β would be expected to move a normal PAD from a peak in Figure 2 to a corresponding peak in the counterstreaming regime of Figure 3 because of a relative decrease in the 90° flux. If β is the driver of the MC PAD trajectories, then those PAD anisotropies would follow the roughly inverse correlation to β of Figure 4 of *Crooker et al.* [2003]. If that is not the case, then the PADs may indeed reflect the MC IMF topologies, which is the accepted interpretation.

[14] An unexpected feature of Figure 3 is the apparent zone of few points along y = x. Relying on directionality to indicate topology, and assuming both closed fields and a roughly inverse relation of loop leg length to flux intensity [*Pilipp et al.*, 1987], then loop geometry may skew the PAD directionalities: A symmetric loop [*Lepping et al.*, 1990, Figure 7] may result in more symmetric CSEs, whereas a loop skewed along the Parker spiral [*Crooker et al.*, 1998a, Figure 5] may skew the directionality distribution as observed. Minimum variance analysis [*Klein and Burlaga*, 1982; *Lepping et al.*, 1990] supports the latter geometry. Alternatively, the fields of Figure 3 may be predominantly open, which removes any expectation of PADs along y = x. Imbalances in footpoint conditions [*Gosling et al.*, 2004] may also affect the counterstreaming ratios; however, why this effect would skew, rather simply broaden, a CSE peak

is unclear. *Gosling et al.* [2001] reported electron PADs that exhibit deep depletions at 90°. These distributions have an appearance similar to CSEs however those authors did not suggest such distributions are necessarily found on closed field lines. These distributions tend to lie within the CSE quadrant of our parameterization plots but it is not clear if they are responsible for "blurring" a potential distinction between open and closed fields.

[15] The counterstreaming HF electron signature is perhaps the leading tool to detect the closed IMF topologies and has been widely used in many analyses of ICMEs [e.g., *Gosling et al.*, 1992; *Gosling and Forsyth*, 2001]. Very clear examples of episodes of HF electron counterstreaming in near simultaneity with other ICME signatures [e.g., *Gosling and Forsyth*, 2001; *Reisenfeld et al.*, 2003] appear to validate the concept. Unfortunately, in practice the counterstreaming tool is perhaps the least quantitative and most subjective of those tools, with counterstreaming epochs selected by eye from color-coded PAD intensity plots. The synoptic and parametric views of HF electron PADs in Figures 2 and 3 show no obvious natural boundaries or limits in parameter space that would allow us to define a counterstreaming criterion that faithfully maps only to closed IMF topologies. However, this result should be pursued with more complex and comprehensive studies of counterstreaming in ICMEs before we can hope to understand the physics that gives rise to the basic differences between the directionality distributions of Figures 2 and 3.

[16] **Acknowledgment.** This research was supported by NASA under grants NAG5-12862 to the University of California, NAG5-10856 to Boston University and by NASA interagency transfer W-19926 to AFRL.

References

Burlaga, L. F. (1991), Magnetic clouds, in *Physics of the Inner Heliosphere II*, edited by R. Schwenn and E. Marsch, p. 1, Springer-Verlag, New York.

Collier, M. R., et al. (2001), Reconnection remnants in the magnetic cloud of October 18–19, 1995: A shock, monochromatic wave, heat flux dropout, and energetic ion beam, *J. Geophys. Res.*, *106*, 15,985.

Crooker, N. U., et al. (1996), Solar wind streamer belt structure, *J. Geophys. Res.*, *101*, 24,331.

Crooker, N. U., J. T. Gosling, and S. W. Kahler (1998a), Magnetic clouds at sector boundaries, *J. Geophys. Res.*, *103*, 301.

Crooker, N. U., et al. (1998b), Sector boundary transformation by an open magnetic cloud, *J. Geophys. Res.*, *103*, 26,859.

Crooker, N. U., D. E. Larson, S. W. Kahler, S. M. Lamassa, and H. E. Spence (2003), Suprathermal electron isotropy in high-beta solar wind and its role in heat flux dropouts, *Geophys. Res. Lett.*, *30*(12), 1619, doi:10.1029/2003GL017036.

Feldman, W. C., J. R. Asbridge, S. J. Bame, M. D. Montgomery, and S. P. Gary (1975), Solar wind electrons, *J. Geophys. Res.*, *80*, 4181.

Gosling, J. T., and R. J. Forsyth (2001), CME-driven solar wind disturbances at high heliographic latitudes, *Space Sci. Rev.*, *97*, 87.

Gosling, J. T., D. N. Baker, S. J. Bame, W. C. Feldman, R. D. Zwickl, and E. J. Smith (1987), Bidirectional solar wind electron heat flux events, *J. Geophys. Res.*, *92*, 8519.

Gosling, J. T., R. M. Skoug, and W. C. Feldman (2001), Solar wind electron halo depletions at 90° pitch angle, *Geophys. Res. Lett.*, *28*, 4155.

Gosling, J. T., D. J. McComas, J. L. Phillips, and S. J. Bame (1992), Counterstreaming solar wind halo electron events: Solar cycle variations, *J. Geophys. Res.*, *97*, 6531.

Gosling, J. T., C. A. de Koning, R. M. Skoug, J. T. Steinberg, and D. J. McComas (2004), Dispersionless modulations in low-energy solar electron bursts and discontinuous changes in the solar wind electron strahl, *J. Geophys. Res.*, *109*, A05102, doi:10.1029/2003JA010338.

Kahler, S., and R. P. Lin (1994), The determination of interplanetary magnetic field polarities around sector boundaries using $E > 2$ keV electrons, *Geophys. Res. Lett.*, *21*, 1575.

Kahler, S. W., and R. P. Lin (1995), An examination of directional discontinuities and magnetic polarity changes around interplanetary sector boundaries using $E > 2$ keV electrons, *Sol. Phys.*, *161*, 183.

Kahler, S., N. U. Crooker, and J. T. Gosling (1998), Properties of interplanetary magnetic sector boundaries based on electron heat-flux flow directions, *J. Geophys. Res.*, *103*, 20,603.

Kahler, S., N. U. Crooker, and J. T. Gosling (1999), The polarities and locations of interplanetary coronal mass ejections in large interplanetary magnetic sectors, *J. Geophys. Res.*, *104*, 9919.

Kahler, S. W., N. U. Crooker, and D. E. Larson (2003), Parameterizing the Wind 3DP heat flux electron data, in *Solar Wind Ten*, *AIP Conf. Proc.*, vol. 679, edited by M. Velli et al., p. 172, Am. Inst. of Phys., Melville, N. Y.

Klein, L. W., and L. F. Burlaga (1982), Interplanetary magnetic clouds at 1 AU, *J. Geophys. Res.*, *87*, 613.

Larson, D. E., R. P. Lin, and J. Steinberg (2000), Extremely cold electrons in the January 1997 magnetic cloud, *Geophys. Res. Lett.*, *27*, 157.

Lepping, R. P., J. A. Jones, and L. F. Burlaga (1990), Magnetic field structure of interplanetary magnetic clouds at 1 AU, *J. Geophys. Res.*, *95*, 11,957.

Lepping, R. P., et al. (1995), The WIND magnetic field investigation, *Space Sci. Rev.*, *71*, 207.

Lin, R. P., et al. (1995), A three dimensional plasma and energetic particle investigation for the wind spacecraft, *Space Sci. Rev.*, *71*, 122.

Marsch, E. (1991), Kinetic physics of the solar wind plasma, in *Physics of the Inner Heliosphere*, vol. 2, edited by R. Schwenn and E. Marsch, p. 45, Springer-Verlag, New York.

Marsden, R. G., T. R. Sanderson, C. Tranquille, K.-P. Wenzel, and E. J. Smith (1987), ISEE 3 observations of low-energy proton bidirectional events and their relation to isolated interplanetary magnetic structures, *J. Geophys. Res.*, *92*, 11,009.

McComas, D. J., J. T. Gosling, J. L. Phillips, S. J. Bame, J. G. Luhmann, and E. J. Smith (1989), Electron heat flux dropouts in the solar wind: Evidence for interplanetary magnetic field reconnection?, *J. Geophys. Res.*, *94*, 6907.

Pilipp, W. G., H. Miggenrieder, K.-H. Muhlhauser, H. Rosenbauer, R. Schwenn, and F. M. Neubauer (1987), Variations of electron distribution functions in the solar wind, *J. Geophys. Res.*, *92*, 1103.

Reisenfeld, D. B., et al. (2003), Properties of high-latitude CME-driven disturbances during Ulysses second northern polar passage, *Geophys. Res. Lett.*, *30*(19), 8031, doi:10.1029/2003GL017155.

Richardson, I. G., and D. V. Reames (1993), Bidirectional ~1 MeV amu^{-1} ion intervals in 1973–1991 observed by the Goddard Space Flight Center instruments on IMP 8 and ISEE 3/ICE, *Astrophys. J. Suppl. Ser.*, *85*, 411.

Richardson, I. G., V. M. Dvornikov, V. E. Sdobnov, and H. V. Cane (2001), Bidirectional cosmic ray and ~1 MeV ion flows, and their association with ejecta, *Proc. Int. Cosmic Ray Conf.*, 3498.

Shodhan, S., et al. (2000), Counterstreaming electrons in magnetic clouds, *J. Geophys. Res.*, *105*, 27,261.

Stansberry, J. A., J. T. Gosling, M. F. Thomsen, and S. J. Bame (1988), Interplanetary magnetic field orientations associated with bidirectional electron heat fluxes detected at ISEE 3, *J. Geophys. Res.*, *93*, 1975.

Tsurutani, B. T., and R. P. Lin (1985), Acceleration of >47 keV ions and >2 keV electrons by interplanetary shocks at 1 AU, *J. Geophys. Res.*, *90*, 1.

N. U. Crooker, Center for Space Physics, Boston University, 725 Commonwealth Ave., Boston, MA 02215, USA.

W. M. Feuerstein, D. E. Larson, R. P. Lin, and J. G. Luhmann, Space Sciences Laboratory, University of California, Berkeley, CA 94720, USA. (michf@ssl.berkeley.edu)

S. W. Kahler, Air Force Research Laboratory, 29 Randolph Road, Building 1110, Hanscom AFB, MA 01731-3010, USA.